# White-rot fungus Phanerochaete chrysosporium metabolizes chloropyridinyl-type neonicotinoid insecticides by an N-dealkylation reaction catalyzed by two cytochrome P450s

Title:

# White-rot fungus *Phanerochaete chrysosporium* metabolizes chloropyridinyl-type neonicotinoid insecticides by an *N*-dealkylation reaction catalyzed by two cytochrome P450s

Authors

Toshio Mori[a], Haruka Ohno[a], Hirofumi Ichinose[b], Hirokazu Kawagishi[acd], Hirofumi Hirai[ac]*

[a] Faculty of Agriculture, Shizuoka University, 836 Ohya, Suruga-ku, Shizuoka 422-8529, Japan

[b] Faculty of Agriculture, Kyushu University, 6-10-1 Hakozaki, Higashi-ku, Fukuoka 812-8581, Japan

[c] Research Institute of Green Science and Technology, Shizuoka University, 836 Ohya, Suruga-ku, Shizuoka 422-8529, Japan

[d] Graduate School of Science and Technology, Shizuoka University, 836 Ohya, Suruga-ku, Shizuoka 422-8529, Japan

* Corresponding author: H. Hirai (e-mail address: hirai.hirofumi@shizuoka.ac.jp)

**Abstract**

We previously identified a cytochrome P450 (CYP) derived from the white-rot fungus *Phanerochaete chrysosporium* as involved in degradation of acetamiprid, a neonicotinoid (NEO) insecticide. In the present study, we investigated biodegradation of other NEOs by *P. chrysosporium*, and attempted to identify the CYP enzyme responsible for NEO degradation. *P. chrysosporium* was able to degrade some NEOs (acetamiprid, clothianidin, imidacloprid, and thiacloprid) in nutrient-rich medium. Degradation was inhibited by the addition of a CYP inhibitor. Two CYPs in *P. chrysosporium* (PcCYPs), CYP5037B3 and CYP5147A3, were identified as major isozymes involved in metabolism of three neonicotinoids that have in common a chloropyridinyl moiety (acetamiprid, imidacloprid, and thiacloprid) by screening yeast that heterologously express PcCYPs. Both PcCYPs catalyzed cleavage of the chloropyridinyl moiety and side chain of the three NEOs by *N*-dealkylation, resulting in 6-chloro-3-pyridinemethanol and respective side chain fragments. In a culture of *P. chrysosporium*, 97% and 74% of imidacloprid and thiacloprid were modified to form degradation products, and one of these, 6-chloro-3-pyridinemethanol, was further degraded. These two PcCYPs catalyzed almost the same reaction but their substrate specificity and expression pattern are slightly different. Altogether, we found that *P. chrysosporium* degrades NEOs via the activity of at least two different CYP isozymes.

**Keywords**

bioremediation, neonicotinoids, *Phanerochaete chrysosporium*, cytochrome P450

**Highlights**

*Phanerochaete chrysosporium* is able to degrade four neonicotinoid insecticides.

Two cytochrome P450 isozymes are involved in degradation of neonicotinoids.

These enzymes react with all chloropyridinyl neonicotinoids tested except nitenpyram.

The degradation reactions are probably carried out via *N*-dealkylation.

## 1. Introduction

Neonicotinoids (NEOs) are insecticides that have in common a nicotine-related molecular structure. NEOs are very commonly used insecticides in various countries, and are very effective because of their transferability to plants, water solubilities, and residual effectiveness. The first NEO, imidacloprid (IMI), appeared in the 1980s and was followed by the development of several IMI analogues. NEOs act as exogenous agonists of nicotinic acetylcholine receptors (nAChRs) and show high affinity to insect nAChRs (Tomizawa and Casida, 2003). Indeed, NEOs exhibit activity against a broad spectrum of invertebrates by continuously stimulating neural transmission in the central nervous system. NEOs usually show a lower affinity for mammalian nAChRs than for insect nAChRs (e.g. (Tomizawa et al., 2000)), such that these compounds show higher selective toxicity to invertebrates. NEOs are used for a wide range of pest control applications, including for the control of important crop, soil, timber, and animal pests.

Contrary, such a broad spectrum of insecticidal activity can also be a disadvantage because NEOs also affect non-target insects. Whitehorn et al. have suggested that for bumble bees, NEOs have a considerable negative impact on colony growth rates and production of new queens (Whitehorn et al., 2012). Moreover, NEOs have impacts on nontarget invertebrates such as butterflies, moths, wasps, beetles, earthworms, and aquatic invertebrates, as reviewed by Pisa et al. (Pisa et al., 2015). As described above, NEOs display lower toxicity against mammals as compared with insects; however, these compounds are known to nonetheless exert direct and

21 indirect negative effects on a wide range of vertebrates (Gibbons et al., 2015). For example,
22 thiacloprid (THI) and thiamethoxam (THX) are considered likely to be human carcinogens and
23 acetamiprid (ACE), and IMI are toxic to birds and fish (Tomizawa and Casida, 2005).
24 Moreover, these metabolites clearly show toxic effects in mammals. The metabolites (a desnitro
25 metabolite of IMI, descyano and olefin analogue type metabolites of THI) showing high affinity
26 against human nAChR showed lethal toxicity to mice, similar to nicotines (epibatidine and
27 nicotine) (Tomizawa et al., 2000). Therefore, some of NEOs metabolites possibly show
28 nicotine-like effect to mammals including human.

29 Therefore, the use of NEOs has been limited in several countries. In 2013, the
30 European Union partially banned the use of three NEOs, IMI, clothianidin (CLO), and THX, in
31 an effort to protect honey bees and other pollinators, then totally banned outdoor use in 2018.
32 Invalidation of THI was decided in 2019, and dinotefuran (DIN) and nitenpyram (NIT) have
33 never been approved until now. At this time, only ACE has avoided imposition of legal controls.
34 In France, use of five NEOs (ACE, CLO, IMI, THI and THX) has already been disallowed in
35 2018. However, NEOs are still used in a variety of countries. As a result of these issues,
36 studying the environmental fate of NEOs has been attracting interest as a research topic. NEOs
37 spread via runoff or dust, and contaminate soil and water in agricultural and nearby areas after
38 use (Bonmatin et al., 2015). Moreover, in some environments (sandy and clay loam soils) NEOs
39 are absorbed into soil and their half-lives can reach 1,000 days (Goulson, 2013). Although
40 NEOs can persist and accumulate in natural environments, soil or water ecosystems are surely

capable of degrading some parts of contaminating NEOs. THX in particular shows low nAChR binding activity and is known as a 'CLO precursor,' as THX in soil is mainly converted to CLO, along with other metabolites (Nauen et al., 2003). Several bacteria able to degrade NEOs have already been isolated from nature, and the corresponding mechanisms and degradation pathways have also been elucidated in part (Hussain et al., 2016). However, information about biodegradation of NEOs by bacteria remains limited, except for IMI. Furthermore, studies of fungal degradation of NEOs are even more limited. Altogether, this indicates the importance of developing microorganisms capable of degrading NEOs, and in particular ACE, CLO, IMI and THI, in order to establish bioremediation applications for removal of NEOs from contaminated environments.

White-rot fungi are well known due to their unique ability to degrade lignin which is one of major wood components. lignin is a recalcitrant aromatic polymer with bearing on wood strength and generally tolerant of biological attack. White-rot fungi have not only lignin-degradation activity but also are able to degrade various recalcitrant organic pollutants (Gao et al., 2010; Pointing, 2001). Our research group has been evaluating the possibility of using white-rot fungi for bioremediation. We have already reported on biodegradation of NEOs (ACE, CLO, NIT and DIN) by the white-rot fungus *Phanerochaete sordida*, including data on the metabolic products and their toxicity (Mori et al., 2017; Wang et al., 2012, 2019b). Overall, we have found that cytochrome P450 enzymes play important roles in NEO degradation reactions in white-rot fungi**.** Additionally, we have reported the identification of fungal CYP

isozymes involved in ACE degradation using the typical white rot fungus *Phanerochaete chrysosporium* (Wang et al., 2019a). Although a dealkylation reaction catalyzed by CYPs might have been carried out as the main reaction bringing about ACE degradation by both fungi, the structures of the metabolic products differed. *N*-demethylation of ACE occurred in the case of metabolism by *P. sordida,* converting ACE to (*E*)-$N^1$-[(6-chloro-3-pyridyl)-methyl]-$N^2$-cyanoacetamidine (Wang et al., 2012), whereas 6-chloropyridine methanol was obtained as a metabolite from culture of *P. chrysosporium* in the presence of ACE (Wang et al., 2019a). This suggests the possibility that the reaction mechanisms for NEO metabolism (other than ACE) and the specific CYP isozymes involved in NEO metabolism might also be different between these fungi. In the present study, we investigated the reactivity of *P. chrysosporium* to NEOs and identified the metabolites resulting from degradation by this fungal species. We also identified the CYP isozymes involved in the NEO-degrading metabolic reactions, shedding light on the mechanisms of degradation of NEOs by white-rot fungi.

## 2. Materials and methods

### *2.1. Strains and chemicals*

*P. chrysosporium* ME446 (ATCC 34541) was kept on potato dextrose agar (PDA) medium at 4°C. The *P. chrysosporium* CYP (PcCYP) expression library used in the screen to select CYPs responsible for NEOs metabolism was constructed previously (Hirosue et al., 2011).

*Saccharomyces cerevisiae* AH22 transformants heterologously expressing PcCYPs were stored at -80°C until use. ACE was obtained from KANTO CHEMICAL Co., Inc., and other NEOs (CLO, DIN, IMI, NIT and THI) were purchased from FUJIFILM Wako Pure Chemical Co. All NEOs used were pesticide residue analysis grade (> 98% purity). 6-Chloro-3-pyridynlmethanol (**I**), 2-nitroamino-2-imidazoline (**III**) and 6-chloro-3-pyridinemethanol (**IV**) were obtained from Tokyo Chemical Industry Co., Ltd.

*2.2. Biodegradation of NEOs by P. chrysosporium*

Two mycelium pellets (1 cm diameter) of *P. chrysosporium* grown on a PDA plate at 30°C were inoculated into a 100-ml Erlenmeyer flask containing 10 ml potato dextrose broth (PDB, Difco). After 5 days of preincubation, 100 µl of NEOs or their metabolic products in solution (10 mM in dimethyl sulfoxide) were added to each culture flask (final concentration: 0.1 mM). After the prescribed incubation period (1 to 4 weeks), the reaction was stopped by addition of an equal amount of methanol, followed by homogenization. For quantification of residual NEOs concentration, the homogenate was centrifuged (10,000 × *g* for 10 min, at 4°C), then filtered (0.2 µm membrane filter) for quantification analysis using high-performance liquid chromatography (HPLC), to quantify NEO remaining. HPLC analysis was performed using a JASCO PU-2089 pump with an MD-2018 photodiode array detector (HPLC-PDA), fitted with an Inertsil ODS-3 column (4.6 × 250 mm, GL Science). The eluent used was 30% methanol aq. at 1 ml/min flow rate. Autoclaved fungal cultures were used as controls.

To evaluate the effects of a CYP inhibitor, we used 1-aminobenzotriazole (1-ABT). A solution of 1-ABT (0 to 100 mM in DMSO) was added to the culture at the time of NEOs addition to adjust the concentration to 0, 0.01, or 0.1 mM. After 2 weeks (for IMI) or 4 weeks of incubation, recovery of NEOs was determined as described above.

*2.3. Degradation of NEOs by recombinant PcCYP-expressing yeasts*

NEO degradation experiments using PcCYP-expressing yeast (*Saccharomyces cerevisiae* strain SH22) were performed as described in previous reports (Hirosue et al., 2011; Wang et al., 2019a). For screening, the yeast strains were separately cultured in 96-deep well plates containing 0.5 ml synthetic dextrose liquid medium with 0.5 mM substrate in each well. Next, the reaction was stopped by adding methanol/acetone and centrifugated, and then the supernatant was filtered for HPLC analysis. To characterize selected PcCYPs, a recombinant yeast suspension prepared from SDL pre-culture was inoculated into 10 ml of newly SDL, along with 100 μl of 10 mM NEOs/DMSO solution (final concentration: 0.1 mM). After incubation for 3 days at 30°C, 200 rpm, the reaction was stopped by the addition of 10 ml methanol. The supernatant was collected following centrifugation (10,000 × *g* for 10 min, at 4°C) and filtrated for HPLC analysis using a membrane filter (0.2 μm). HPLC analysis was performed as described above to quantify the amount of NEO and metabolites. If necessary, the supernatant was concentrated prior to HPLC analysis. Yeast transformed with a version of the pGYR vector containing a GFP gene instead of *PcCYP*s was used as the control strain.

*2.4. Identification of degradation products*

Supernatant obtained from yeast culture reacted with NEOs was extracted with ethyl acetate. The organic layer was evaporated and dissolved in methanol. The metabolite contained in the extract was isolated by preparative HPLC using a Develosil C30 UG-5 column (20 × 250 mm, Nomura Chemical Co., Ltd.). The eluent used was 15% or 30% methanol aq. at 5 ml/min flow rate. Newly isolated metabolites were provided for HPLC-PDA, GC-MS, ESI-MS and/or $^{1}$H-NMR analyses. GC-MS was performed using a Shimadzu gas chromatograph-mass spectrometer (Shimadzu Co.) equipped with a Rtx®-5MS capillary column (3.0 m × 0.25 mm × 0.25 μm, GL sciences, Tokyo, Japan). ESI-MS and NMR analyses were done using a JMS-T100LC mass spectrometer (JEOL Ltd.) or JEOL Lambda-500 spectrometer (JEOL Ltd.), respectively. Metabolites of IMI and THI obtained from fungal cultures in flasks were identified by comparison with the retention time and UV-spectrum of authentic standards by HPLC analysis.

*2.5. Analysis of expression of PcCYPs responsible for NEOs metabolism*

*P. chrysosporium* was cultivated in PDB medium as described above. After 5 days of cultivation and every additional week, mycelium was recovered from each flask. Total RNA extraction from the mycelium, purification, and on-column DNA digestion was performed using an Rneasy Mini Kit (Qiagen) and RNase-free DNase set (Qiagen), then cDNA was synthesized

141 from 200 ng of total RNA using a PrimeScript RT-PCR kit (TaKaRa Bio Inc.). TaKaRa ExTaq
142 DNA polymerase was used for reverse transcription (RT)-PCR with specific primers for actin
143 (5'-aaggactcttacgtcggtgatg-3' and 5'-atcttctcacggttagccttgg-3', amplicon size; 209 bp),
144 CYP5147A3 (5'-agcttggctttaccgtctagc-3' and 5'-ttactaaacaagaaagagtcgccg-3', amplicon size;
145 1581 bp) and CYP5037B3 (5'-tctgccatgctgttgtttgc-3' and 5'-tgcatcatcgcccagacatt-3', amplicon
146 size; 1178 bp). The reaction was begun with denaturation at 95°C for 30 sec, and 26 (for actin)
147 or 28 (for PcCYPs) cycle reactions were performed. Reaction cycles were repeated as follows:
148 95°C for 10 sec, 65°C (actin) or 60°C (PcCYPs) for 10 sec, 72°C for 20 sec (actin) or 80 sec
149 (PcCYPs). Subsequently, a final extension was done at 72°C for 2 min. Unless otherwise noted,
150 all experimental procedures were done following the product manufacturer's protocols. Since it
151 was difficult to design primers for quantitative RT-PCR of PcCYPs, RT-PCR products were
152 then run on a 0.7% agarose gel and the intensity of the bands were semi-quantified using
153 ImageJ software (Abràmoff et al., 2004). The relative expression levels of both CYP genes were
154 expressed using actin as reference.

155 Mycelium of *P. chrysosporium* were obtained from PDB cultures by filtration after
156 preincubation and every additional week. Obtained mycelium was dried at 105 ºC, then
157 weighted. Residual concentration of reducing sugars in filtrate was measured by
158 Somogyi-Nelson method (Somogyi, 1952).

159

160 **3. Results and Discussion**

*3.1. Biodegradation of NEOs by P. chrysosporium*

Previously, we reported the biodegradation of ACE by *P. chrysosporium* and identified CYP5147A3 as an enzyme responsible for ACE metabolism, based on activity screening of PcCYPs heterologously expressed in *S. cerevisiae* (Wang et al., 2019a). In the study, we also identified 6-chloro-3-pyridylmethanol and *N'*-cyano-*N*-methyl acetamidine as ACE metabolites from both *P. chrysosporium* and recombinant yeast cultures. In the present study, we investigated biodegradation by *P. chrysosporium* of a panel of NEOs, namely CLO, DIN, IMI, NIT, THI and ACE. No remarkable degradation of DIN or NIT by *P. chrysosporium* was observed. The results of a time-course analysis of degradation of ACE, CLO, IMI and THI are shown in Fig. 1. Control experiments using autoclaved *P. chrysosporium* did not show any NEOs degradation during 4-week incubation. ACE degradation was only observed at a later cultivation stage, with just a slight amount (less than 5%) degraded during the 2 weeks incubation period, but 27.5% degraded at 4 weeks of incubation. The time course of CLO degradation was almost the same as that observed for ACE, i.e. 28% of CLO was degraded at 4 weeks of incubation. Degradation of IMI began in the first 7-day cultivation period and the degradation rate for IMI increased over time. During the first week, 13.7% of IMI disappeared from the culture, 31.8% was degraded in next a week, and 49.8% was degraded in 3rd week. At 4 weeks, IMI was completely degraded. THI degradation was much slower than what was observed for IMI, and the time course of THI degradation was between that of ACE and IMI/CLO. Thus, the time courses of degradation of each NEO showed a different pattern,

suggesting that degradation of each NEO by *P. chrysosporium* is caused by different enzymes. Therefore, we presumed that there are other PcCYPs involved in degradation of NEOs, i.e. additional to CYP5147A3, which is responsible for ACE degradation (Wang et al., 2019a).

To evaluate the effects of a CYP inhibitor on degradation of NEOs, we added 1-ABT and NEOs (ACE, CLO, IMI and THI) to the fungal culture at the same time. After incubation for 2 weeks (for IMI) or 4 weeks (for the other NEOs: ACE, THI, and CLO), we observed a gradual inhibition of NEO degradation as indicated by changes in the 1-ABT concentration. These results suggest that PcCYPs are involved in IMI, CLO and THI degradation by *P. chrysosporium*, as with ACE degradation. Although 1-ABT effectively inhibited metabolism of ACE, IMI and THI by *P. chrysosporium*, the inhibition by 1-ABT of CLO degradation was less than for the other 3 NEOs. Additionally, degradation of ACE and THI was sensitive to 1-ABT addition, 0.01 mM 1-ABT inhibited about 60% of ACE and THI degradation. IMI degradation was moderately inhibited by 1-ABT addition. Because different inhibitory effects of 1-ABT for IMI, CLO and ACE/THI degradation by *P. chrysosporium* was observed, it is suggested that different PcCYPs isozyme involves in degradation of each NEOs.

### *3.2. IMI and THI degradation mechanism of P. chrysosporium*

We next conducted functional screens for degradation activity using a library of recombinant PcCYPs heterologously expressed in *S. cerevisiae*. All NEOs other than ACE were used for screening. CYP5147A3 was identified as one of the PcCYPs responsible for

201 degradation of ACE (Wang et al., 2019a). In the present study, CYP5037B3 showed clear IMI
202 degradation, and moderate THI degradation was observed in both CYP5037B3 and
203 CYP5147A3-expressing yeast cultures. For other NEOs, a clear reaction was not observed.
204 Because this screening system using 96-well plates does not have high sensitivity, subsequent
205 functional characterization of selected two PcCYPs was performed in flask-scale. After 3 days
206 of cultivation, ACE, IMI and THI were clearly degraded in both recombinant yeasts expressing
207 CYP5037B3 and CYP5147A3 (Table 1). CYP5037B3 expressing yeast showed higher
208 IMI-degradation activity than CYP5147A3 expressing yeast. Contrary, ACE and THI was more
209 degraded in CYP5147A3 expression yeast culture than CYP5037B3 expressing yeast culture.
210 Although CLO degradation by *P. chrysosporium* was inhibited by the addition of a CYP
211 inhibitor, neither yeast strain showed metabolic activities against CLO. This result suggests that
212 PcCYPs other than CYP5037B3 and CYP5147A3 are responsible for degradation of CLO in *P.*
213 *chrysosporium*. And the activities of PcCYPs responsible to CLO degradation might not be
214 successfully expressed in the presented yeast expression system. In addition, we found that
215 neither DIN nor NIT was degraded by either yeast strain expressing PcCYPs. This result is
216 consistent with our finding that *P. chrysosporium* was not able to degrade DIN or NIT.

217 HPLC analyses revealed that ACE, CLO, IMI and THI were clearly degraded in both
218 yeast cultures. For ACE, we observed that 51.0 and 92.5 μM of ACE was degraded in
219 CYP5037B3 and CYP5147A3 expressing yeast cultures, respectively. In addition, the same two
220 metabolites (**I** and **II**, retention time (RT) = 4.7 min and 9.7 min, respectively) were detected

221 from both recombinant yeast cultures containing ACE following HPLC analysis of these
222 extracts. Metabolites of ACE that react with CYP5147A3 have already been identified
223 previously, and including 6-chloro-3-pyridylmethanol and 2-nitroamino-2-imidazoline (Wang et
224 al., 2019a). Thus, it was clear that in addition to CYP5147A3, CYP5037B3 also catalyzes
225 *N*-dealkylation of ACE. While only 14.1 μM of IMI was degraded by CYP5147A3-expressing
226 yeast during a 3-day incubation, CYP5037B3 expression yeast exhibited higher IMI-degrading
227 activity (67.5 μM). We detected 6-chloro-3-pyridylmethanol (**I**) and metabolite **III** (RT=3.7
228 min) in both culture extracts of CYP5037B3 and CYP5147A3-expressing yeasts. Metabolite **III**
229 showed mass spectra at *m/z* 129 ($M^+$-H) on negative ion mode, and 131 ($M^+$+H) and 153 ($M^+$-H,
230 +Na) on positive ion mode on ESI-MS, and the molecular mass of metabolite **III** was
231 determined to be 130. The $^1$H-NMR spectrum of metabolite **III** had only one doublet peak at
232 3.71 ppm in $CD_3OD$. These spectra indicated that metabolite **III** is a fragment of the side chain
233 region of IMI. Based on these results, as well as a comparison of the retention time and
234 UV-spectrum on HPLC-PDA analysis with the authentic standard, we identified metabolite **III**
235 as 2-nitroamino-2-imidazoline. Three metabolites of THI (metabolites **I**, **IV** (RT=4.7 min) and
236 **V** (RT=15.0 min)) were obtained from the culture extract of CYP5147A3-expressing yeast.
237 Metabolite **V** was only detectable when a concentrated extract was analyzed by HPLC. By
238 contrast, only metabolites **I** and **IV** were detected in a culture of CYP5037B3-expressing yeast.
239 On ESI-MS analysis, metabolite **IV** showed molecular ions *m/z* 128 ($M^+$+H) and 150 ($M^+$+Na)
240 on positive ion mode. By comparing these findings with the retention time and UV-spectrum of

241 an authentication standard by HPLC-PDA analysis, metabolite **IV** was identified as
242 2-cyanoimino-1,3-thiazolidine. Metabolite **V** is a minor metabolite that required concentration
243 for detection by HPLC. The ESI-MS spectrum of isolated **V** showed a molecular ion at *m/z* 271
244 on positive ion mode, and an ion peak at *m/z* 293 ($M^+$-H, +Na) was also observed. Both ions
245 were accompanied by +2 mass chlorine isotope peaks. From the mass spectrum and $^1$H- and
246 $^{13}$C-NMR spectra in $CD_3OD$ (shown in Table 2), metabolite **V** was identified as thiacloprid
247 amide (THI-amide) (Dai et al., 2010).

248 As shown in Table 1, the yields of metabolite **I** were over 80% of degraded ACE,
249 IMI and THI in cultures of yeast expressing CYP5037B3. Although recovery of metabolite **II**
250 could not be determined because there is no authentic standard, yeast expressing CYP5037B3
251 also exhibited a high rate of conversion of IMI and THI to side-chain fragments **III** and **IV**
252 (around 93% or more). The conversion rates of ACE and IMI by yeast expressing CYP5147A3
253 were nearly the same as that observed for CYP5037B3. However, the rates of conversion of
254 THI to **I** and **IV** by CYP5147A3 were slightly lower than others. The reason seems to be that
255 CYP5147A3 is able to catalyze two reactions to form two major metabolites **I**, **IV** or a minor
256 metabolite **V**. In Fig. 3, we present a summary of degradation of NEOs and metabolite
257 production. Both CYP5037B3 and CYP5147A3 are likely to have almost the same catalytic
258 mechanism. All metabolites, except metabolite **V** (THI-amide), were produced via
259 *N*-dealkylation.

260 Some functions of these PcCYPs have been reported previously. For example,

261 CYP5037B3 catalyzes *O*-dealkylation of 7-ethoxycoumarin, and CYP5147A3 catalyzes
262 *S*-oxidation of dibenzothiophene, 11β-hydroxylation of testosterone, as well as *O*-dealkylation
263 of 7-ethoxycoumarin (Ichinose, 2013). Although CYP5147A3 shows a broad range of substrate
264 specificity, both of the PcCYPs might share a catalytic mechanism with regards to the
265 *O*-dealkylation reaction. In the present study, both PcCYPs catalyzed the reaction with identical
266 NEOs as substrates and produced same *N*-dealkylation products. Accordingly, we propose that
267 both CYP5037B3 and CYP5147A3 catalyze the *N*-dealkylation reaction of ACE, IMI and THI
268 via the same mechanism, which might be either a hydrogen atom transfer or a single electron
269 transfer (Wang et al., 2019a). In addition, we suggest that the chloropyridinyl structure might be
270 important for showing the activity of these PcCYPs, as CYP5037B3 and CYP5147A3 degraded
271 ACE, IMI and THI but not CLO (Fig. 2). However, neither selected PcCYP showed activity
272 against NIT, which has a chloropyridinyl structure. This could be due to the bulky nature and/or
273 electronegativity of the nitrovinyl structure. Additionally, *N*-nitro and *N*-cyanoimine moieties
274 that are critical for binding to nAChR, along with structures of the heterocyclic of acyclic spacer,
275 do not seem to be important for the activity of these PcCYPs (Casida, 2011). THI-amide
276 production was only observed in a culture of CYP5147A3-expressing yeast; this might be
277 attributable to broad substrate specificity of CYP5147A3. Because it has been reported
278 CYP5147A3 can catalyze reaction to broad range substrate by comparison of CYP5037B3, as
279 described above (Ichinose, 2013). However, information of strict substrate specificity of these
280 PcCYPs must be provided by the experiments using purified PcCYPs.

To confirm whether the mechanism of degradation by *P. chrysosporium* is the same as that of recombinant yeasts, we next analyzed metabolites formed from ACE, IMI and THI. Although we note that only a tiny amount of metabolite **I** was obtained from a vast amount of culture extract of *P. chrysosporium* with ACE in a previously study, no accumulation of metabolite **I** from ACE was observed in the present study, as was also true for IMI and THI. When compound **I** was added to the *P. chrysosporium* culture, only 10.0 ± 2.4% of added **I** was recovered after one week of incubation. The result indicates that metabolite **I** is more easily metabolized than the parent compound ACE, IMI or THI. Furthermore, this compound does not accumulate in the culture. Metabolite **II** was clearly produced in a culture of *P. chrysosporium* with ACE, as previously reported (Wang et al., 2019a). Metabolites **III** and **IV** were found by HPLC analysis from fungal culture with IMI and THI, respectively. Although **I** was not detectable in extracts of either culture, 97.0% of degraded IMI and 74.2% of degraded THI in the fungal cultures had been converted to metabolites **III** and **IV**, respectively. **V**, a minor metabolic product of THI in CYP5147A3 expressing yeast, was not observed by HPLC analysis, even though the extract of the fungus culture with THI had been highly concentrated. Therefore, the majority of IMI degradation is probably catalyzed by both PcCYPs to form major metabolite **I** and side-chain fragments (**II**, **III** and **IV**) via *N*-dealkylation, then **I** is further metabolized. On the other hand, we considered two possibilities for the cause of lower recovery of **IV** from THI degradation. The first is further metabolism of **IV** and the other is the involvement of other PcCYPs giving different metabolites. We confirmed degradability of **III** and **IV** in a culture of

*P. chrysosporium*. In this further degradation reaction, 63% of the initial **IV** (100 μM) was degraded during a 2-week incubation; however, only 4% of **III** was degraded. This indicates that *P. chrysosporium* metabolizes THI by a reaction involving CYP5037B3 and CYP5147A3 to form mainly **I** and **IV**, **I** is quickly metabolized, and **IV** is slowly metabolized.

A similar reaction to form 6-chloronicotinic acid (6-CNA) or 6-chloro-3-pyridylmethanol from NEOs with chloropyridinyl structures has been found in mice and spinach, along with several other reactions (Ford and Casida, 2006)(Ford and Casida, 2008). The reports of these activities describe that both products are produced as major metabolites by oxidation (in mice or spinach) or by reduction (spinach) of 6-chloronicotinaldehyde formed from *N*-dealkylation of ACE, IMI, NIT and THI. The metabolism of IMI in several organisms including bacteria, plant and mammals has been particularly well investigated. Schulz-Jander and Casida (Schulz-Jander and Casida, 2002) performed *in vivo* IMI-metabolic reaction with 8 recombinant human CYPs. These human CYPs catalyzed hydroxylation and desaturation of imidazolidine moiety or reduction and elimination of *N*-nitro moiety, however, 6-CNA and 6-chloro-3-pyridylmethanol were not detected in these reactions. That is to say, the enzymes catalyzing direct *N*-dealkylation of NEOs with a chloropyridinyl moiety have not been well understood, such that the findings for fungal CYPs catalyzing direct *N*-dealkylation will be useful information for understanding the mechanisms of metabolism of NEOs in various organisms.

*3.3. Expression analysis of CYP5037B3 and CYP5147A3*

After a 5-day preincubation, total RNA was extracted from a culture of *P. chrysosporium* subjected to additional 0- to 4-week incubation periods. The results of expression analysis are shown in Fig. 4. Expression of the actin gene was clearly observed at all incubation periods. Semi-quantitative expression levels of PcCYPs were provided by image processing using ImageJ software. *CYP5037B3* was weakly expressed during 0-1 weeks cultivation and higher expression levels were detected at 2- and 3-week incubation periods. Expression levels then dropped at 4 weeks. *CYP5147A3* showed a much weaker expression at 0- and 1-week cultivation periods, expression levels were increased at the 2nd week, and then levels decreased as the incubation period extended. IMI degradation and CYP5037B3 expression correlated well, as metabolic activity of IMI of CYP5037B3 was much higher than that of CYP5147A3 (Table 1). As shown in Fig. 1, *P. chrysosporium* accelerated ACE and THI degradation after 2 weeks of cultivation, such that ACE and THI degradation seem likely to depend mainly on expression of CYP5147A3.

Dried mycelial weight after pre-incubation, 1- or 2-weeks incubation, were 54.5 ± 2.3, 56.0 ± 0.1 and 42.8 ± 0.3 mg/flask, respectively. *P. chrysosporium* consumed almost half of reducing sugar (47.6% remaining) during preincubation, and most of residual sugars was consumed during additional 1-week incubation (2.6% remaining). From this result, it is expected that *P. chrysosporium* got into nutrient starvation condition during 1-2 weeks incubation period and started autolysis, in PDB culture. In the previous report, *P.*

*chrysosporium* increased the expression of some CYPs associating to secondary metabolism under starvation condition (Doddapaneni and Yadav, 2005). From these facts, it is presumed that CYP5037B3 and CYP5147A3 expressed under starvation condition.

## 4. Conclusion

In the present study, we investigated degradation of several NEOs by the white-rot fungus *P. chrysosporium,* which is able to metabolize acetamiprid via the activity of CYP. We found that this fungus can degrade CLO, IMI and THI in addition to ACE. Metabolic reactions with ACE, IMI and THI, which have in common that they each contain a chloropyridinyl structure, were catalyzed by two PcCYPs to form a common *N*-dealkylated product and respective side-chain fragments. Although no metabolic product of CLO was yet identified, these results show the applicative potential of *P. chrysosporium* for bioremediation of NEOs because the fungus was able to degrade four NEOs that appear to be major pollutants in soil environments. We demonstrated that both CYP5037B3 and CYP5147A3, which were identified as major PcCYPs, are involved in ACE, IMI and THI metabolism, catalyzing direct *N*-dealkylation of these NEOs. By contrast, these PcCYPs were not able to react with CLO, indicating the presence of other PcCYPs involved in CLO degradation. Future work could be focused on the identification of the PcCYPs that catalyze CLO degradation and identification of its metabolites. Although CYPs also play important roles in degradation of NEOs by *P. sordida*, the target NEOs and metabolic products formed by *P. sordida* are completely different from

those we have identified for *P. chrysosporium* (Mori et al., 2017; Wang et al., 2012, 2019a, 2019b). It is possible that the differences in the mechanisms of degradation of individual NEOs by each fungal species result from diversity of CYPs in white-rot fungi (Floudas et al., 2012).

**Declaration of Competing Interest**

The authors declare no competing financial interest.

**CRediT authorship contribution statement**

**Toshio Mori:** Writing - original draft, Visualization. **Haruka Ohno:** Investigation, Visualization. **Hirofumi Ichinose:** Investigation, Resources. **Hirokazu Kawagishi:** Writing - review & editing. **Hirofumi Hirai:** Writing - review & editing, Supervision, Project administration, Funding acquisition.

**Acknowledgement**

This research was supported by a Grant-in-Aid for Scientific Research (B) (Grant No. 15H04618) from the Ministry of Education, Culture, Sports, Science and Technology of Japan.

**References**

Abràmoff, M.D., Magalhães, P.J., Ram, S.J., 2004. Image processing with imageJ. Biophotonics Int. 11, 36–41. http://dx.doi.org/10.1201/9781420005615.ax4.

381 Bonmatin, J.M., Giorio, C., Girolami, V., Goulson, D., Kreutzweiser, D.P., Krupke, C., Liess,
382 M., Long, E., Marzaro, M., Mitchell, E.A., Noome, D.A., Simon-Delso, N., Tapparo, A.,
383 2015. Environmental fate and exposure; neonicotinoids and fipronil. Environ. Sci. Pollut.
384 Res. 22, 35–67. https://doi.org/10.1007/s11356-014-3332-7.
385 Casida, J.E., 2011. Neonicotinoid metabolism: Compounds, substituents, pathways, enzymes,
386 organisms, and relevance. J. Agric. Food Chem. 59, 2923–2931.
387 https://doi.org/10.1021/jf102438c.
388 Dai, Y.J., Ji, W.W., Chen, T., Zhang, W.J., Liu, Z.H., Ge, F., Sheng, Y., 2010. Metabolism of
389 the neonicotinoid insecticides acetamiprid and thiacloprid by the yeast Rhodotorula
390 mucilaginosa strain IM-2. J. Agric. Food Chem. 58, 2419–2425.
391 https://doi.org/10.1021/jf903787s.
392 Doddapaneni, H., Yadav, J.S., 2005. Microarray-based global differential expression profiling
393 of P450 monooxygenases and regulatory proteins for signal transduction pathways in the
394 white rot fungus Phanerochaete chrysosporium. Mol. Genet. Genomics 274, 454–466.
395 https://doi.org/10.1007/s00438-005-0051-2.
396 Floudas, D., Binder, M., Riley, R., Barry, K., Blanchette, R.A., Henrissat, B., Martínez, A.T.,
397 Otillar, R., Spatafora, J.W., Yadav, J.S., Aerts, A., Benoit, I., Boyd, A., Carlson, A.,
398 Copeland, A., Coutinho, P.M., de Vries, R.P., Ferreira, P., Findley, K., Foster, B., Gaskell,
399 J., Glotzer, D., Górecki, P., Heitman, J., Hesse, C., Hori, C., Igarashi, K., Jurgens, J.A.,
400 Kallen, N., Phil, K., Kohler, A., Kües, U., Kumar, T.K.A., Kuo, A., LaButti, K., Larrondo,

401 L.F., Lindquist, E., Ling, A., Lombard, V., Lucas, S., Lundell, T., Martin, R., McLaughlin,
402 D.J., Morgenstern, I., Morin, E., Murat, C., Nagy, L.G., Nolan, M., Ohm, R.A.,
403 Patyshakuliyeva, A., Rokas, A., Ruiz-Dueñas, F.J., Sabat, G., Salamov, A., Samejima, M.,
404 Schmutz, J., Slot, J.C., John, F. St., Stenlid, J., Pisabarro, A., Eastwood, D.C., Martin, F.,
405 Cullen, D., Grigoriev, I. V., Hibbett, D.S., 2012. The Paleozoic Origin of Enzymatic
406 Lignin Decomposition Reconstructed from 31 Fungal Genomes. Science. 336, 1715–1719.
407 https://doi.org/10.1126/science.1221748
408 Ford, K.A., Casida, J.E., 2008. Comparative metabolism and pharmacokinetics of seven
409 neonicotinoid insecticides in spinach. J. Agric. Food Chem. 56, 10168–10175.
410 https://doi.org/10.1021/jf8020909.
411 Ford, K.A., Casida, J.E., 2006. Chloropyridinyl neonicotinoid insecticides: Diverse molecular
412 substituents contribute to facile metabolism in mice. Chem. Res. Toxicol. 19, 944–951.
413 https://doi.org/10.1021/tx0600696.
414 Gao, D., Du, L., Yang, J., Wu, W.-M., Liang, H., 2010. A critical review of the application of
415 white rot fungus to environmental pollution control. Crit. Rev. Biotechnol. 30, 70–77.
416 https://doi.org/10.3109/07388550903427272.
417 Gibbons, D., Morrissey, C., Mineau, P., 2015. A review of the direct and indirect effects of
418 neonicotinoids and fipronil on vertebrate wildlife. Environ. Sci. Pollut. Res. 22, 103–118.
419 https://doi.org/10.1007/s11356-014-3180-5.
420 Goulson, D., 2013. An overview of the environmental risks posed by neonicotinoid insecticides.

J. Appl. Ecol. 50, 977–987. https://doi.org/10.1111/1365-2664.12111.

Hirosue, S., Tazaki, M., Hiratsuka, N., Yanai, S., Kabumoto, H., Shinkyo, R., Arisawa, A., Sakaki, T., Tsunekawa, H., Johdo, O., Ichinose, H., Wariishi, H., 2011. Insight into functional diversity of cytochrome P450 in the white-rot basidiomycete *Phanerochaete chrysosporium*: Involvement of versatile monooxygenase. Biochem. Biophys. Res. Commun. 407, 118–123. https://doi.org/10.1016/j.bbrc.2011.02.121.

Hussain, S., Hartley, C.J., Shettigar, M., Pandey, G., 2016. Bacterial biodegradation of neonicotinoid pesticides in soil and water systems. FEMS Microbiol. Lett. 363. https://doi.org/10.1093/femsle/fnw252.

Ichinose, H., 2013. Cytochrome P450 of wood-rotting basidiomycetes and biotechnological applications. Biotechnol. Appl. Biochem. 60, 71–81. https://doi.org/10.1002/bab.1061.

Mori, T., Wang, J., Tanaka, Y., Nagai, K., Kawagishi, H., Hirai, H., 2017. Bioremediation of the neonicotinoid insecticide clothianidin by the white-rot fungus *Phanerochaete sordida*. J. Hazard. Mater. 321, 586–590. https://doi.org/10.1016/j.jhazmat.2016.09.049.

Nauen, R., Ebbinghaus-kintscher, U., Salgado, V.L., Kaussmann, M., 2003. Thiamethoxam is a neonicotinoid precursor converted to clothianidin in insects and plants. Pestic. Biochem. Physiol. 76, 55–69. https://doi.org/10.1016/S0048-3575(03)00065-8.

Pisa, L.W., Amaral-Rogers, V., Belzunces, L.P., Bonmatin, J.M., Downs, C.A., Goulson, D., Kreutzweiser, D.P., Krupke, C., Liess, M., Mcfield, M., Morrissey, C.A., Noome, D.A., Settele, J., Simon-Delso, N., Stark, J.D., Van der Sluijs, J.P., Van Dyck, H., Wiemers, M.,

2015. Effects of neonicotinoids and fipronil on non-target invertebrates. Environ. Sci. Pollut. Res. 22, 68–102. https://doi.org/10.1007/s11356-014-3471-x.

Pointing, S.B., 2001. Feasibility of bioremediation by white-rot fungi. Appl. Microbiol. Biotechnol. 57, 20–33. https://doi.org/10.1007/s002530100745.

Schulz-Jander, D.A., Casida, J.E., 2002. Imidacloprid insecticide metabolism: human cytochrome P450 isozymes differ in selectivity for imidazolidine oxidation versus nitroimine reduction. Toxicol. Lett. 132, 65–70. https://doi.org/10.1016/S0378-4274(02)00068-1.

Somogyi, M., 1952. Note on sugar determination. J. Biol. Chem. 195, 19–23.

Tomizawa, M., Casida, J.E., 2005. Neonicotinoid insecticide toxicology: Mechanisms of selective action. Annu. Rev. Pharmacol. Toxicol. 45, 247–268. http://dx.doi.org/10.1016/j.biortech.2015.08.031.

Tomizawa, M., Casida, J.E., 2003. Selective toxicity of neonicotinoids attributable to specificity of insect and mammalian nicotinic receptors. Annu. Rev. Entomol. 48, 339–364. https://doi.org/10.1146/annurev.ento.48.091801.112731.

Tomizawa, M., Lee, D.L., Casida, J.E., 2000. Neonicotinoid insecticides: molecular features conferring selectivity for insect versus mammalian nicotinic receptors. J. Agric. Food Chem. 48, 6016–6024. https://doi.org/10.1021/jf000873c.

Wang, J., Hirai, H., Kawagishi, H., 2012. Biotransformation of acetamiprid by the white-rot fungus *Phanerochaete sordida* YK-624. Appl. Microbiol. Biotechnol. 93, 831–835.

461 https://doi.org/10.1007/s00253-011-3435-8.

462 Wang, J., Ohno, H., Ide, Y., Ichinose, H., Mori, T., Kawagishi, H., Hirai, H., 2019a.
463 Identification of the cytochrome P450 involved in the degradation of neonicotinoid
464 insecticide acetamiprid in Phanerochaete chrysosporium. J. Hazard. Mater. 371, 494–498.
465 https://doi.org/10.1016/j.jhazmat.2019.03.042.

466 Wang, J., Tanaka, Y., Ohno, H., Jia, J., Mori, T., Xiao, T., Yan, B., Kawagishi, H., Hirai, H.,
467 2019b. Biotransformation and detoxification of the neonicotinoid insecticides nitenpyram
468 and dinotefuran by Phanerochaete sordida YK-624. Environ. Pollut. 252, 856–862.
469 https://doi.org/10.1016/j.envpol.2019.06.022.

470 Whitehorn, P.R., O'Connor, S., Wackers, F.L., Goulson, D., 2012. Neonicotinoid pesticide
471 reduces bumble bee colony growth and queen production. Science. 336, 351–352.
472 https://doi.org/10.1126/science.1215025

473

474 **Figure captions**

475 **Fig. 1. Time course of degradation of NEOs (ACE, CLO, IMI and THI) in a culture of *P.***
476 ***chrysosporium*.** Degradation rates of ACE (square), CLO (triangle), IMI (circle) and THI
477 (rhombus) in live fungal cultures were indicated as open symbols, and control experiment
478 using autoclave culture were indicate respective closed symbols. Values are means ±
479 standard deviation of samples in triplicate.

480

481 **Fig. 2. Inhibitory effect of a cytochrome P450 inhibitor, 1-ABT, on degradation of ACE,**
482 **CLO, IMI and THI by *P. chrysosporium*.** 1-ABT and NEOs were added at the same time
483 to pre-incubated culture of *P. chrysosporium*. After 4 weeks (for ACE, CLO and THI) or 2
484 weeks (for IMI) of incubation, residual amounts of NEOs were measured on HPLC. Values
485 are means ± standard deviation of samples in triplicate.

486

487 **Fig. 3. Schematic diagram of NEOs metabolic pathways in cultures of *P. chrysosporium,* or**
488 **of yeast expressing CYP5037B3 or CYP5147A3.** Values express the transformation rate
489 as calculated based on the amount of degraded NEOs and recovered metabolites. Asterisk
490 indicates that the reaction was confirmed in previous work (Wang et al., 2019a).

491

492 **Fig. 4. RT-PCR analysis of CYP5037B3, CYP5147A3, and actin expression in 0- to**
493 **4-week-old cultures of *P. chrysosporium*.** Values below images are relative expression

494 levels of PcCYPs semi-quantified using actin as reference gene by ImageJ software

495 (Abràmoff et al., 2004). Relative expression level is expressed by percentage of highest

496 expression (CYP5037B3 expression at week 3).

497

498

Table 1 Degradation of NEOs and metabolite production in cultures of recombinant yeast expressing CYP5037B3 or CYP5147A3

| PcCYPs | NEOs | degradation (μM) | metabolites (μM) | | |
|---|---|---|---|---|---|
| | | | **I** | **II**, **III** or **IV** | other product |
| CYP5037B3 | ACE | 56.7 ± 2.5 | 47.4 ± 0.2 | accumulate[1] | |
| | CLO | < 5.0 | n.d.[2] | n.d.[2] | |
| | IMI | 59.6 ± 0.2 | 54.9 ± 0.9 | 57.4 ± 1.1 | |
| | THI | 53.2 ± 0.7 | 42.7 ± 2.8 | 49.4 ± 0.7 | |
| CYP5147A3 | ACE | 97.3 ± 0.5 | 85.8 ± 1.2 | accumulate[1] | |
| | CLO | < 5.0 | n.d.[2] | n.d.[2] | |
| | IMI | 14.6 ± 1.1 | 12.1 ± 0.3 | 13.8 ± 0.7 | |
| | THI | 73.9 ± 1.4 | 57.4 ± 0.4 | 65.6 ± 0.8 | **V** (THI-amide) |

The values are means ± standard deviation of triplicated samples.

[1] Metabolic product II was clearly accumulated in both yeast cultures, however, the amount has not determined because no standard.

[2] n.d. means “not detectable”.

Table 2 $^{1}H$- and $^{13}C$-NMR spectra for THI-amide (in $CD_3OD$)

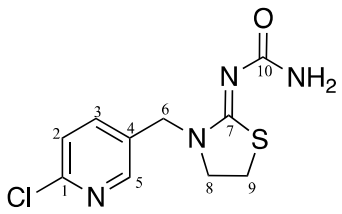


| Position | $^{13}C$ | $^{1}H$ |
|---|---|---|
| | $\delta_C$ | $\delta_H$ |
| 1 | 151.5 | - |
| 2 | 125.7 | 7.44 (d), 1H, *J*= 8.0 Hz |
| 3 | 141.0 | 7.82 (dd), 1H, $J_1$= 8.6 Hz, $J_2$= 2.3 Hz |
| 4 | 133.4 | - |
| 5 | 150.5 | 8.36 (d), 1H, *J*= 2.9 Hz |
| 6 | 48.0 | 4.79 (s) |
| 7 | 171.5 | - |
| 8 | 27.6 | 3.60 (t), 2H, *J*= 7.8 Hz |
| 9 | 50.5 | 3.12 (t), 2H, *J*= 7.5 Hz |
| 10 | 166.9 | - |

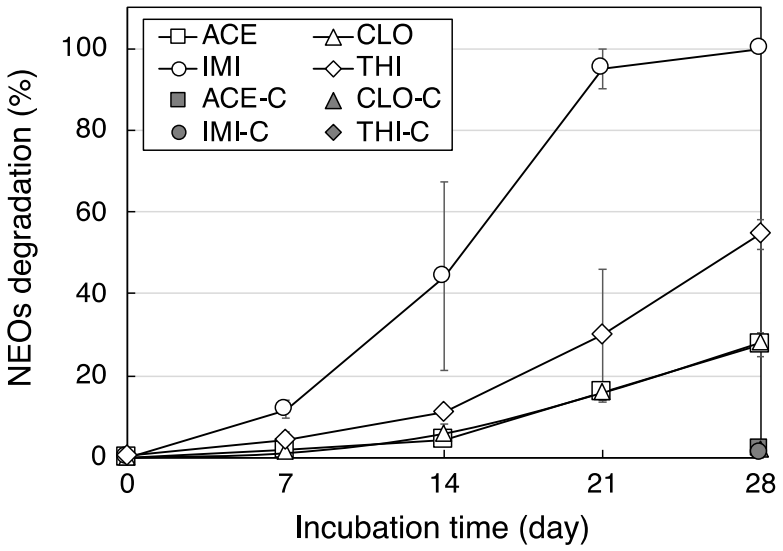


**Fig. 1. Time course of degradation of NEOs (ACE, CLO, IMI and THI) in a culture of *P. chrysosporium*.** Degradation rates of ACE (square), CLO (triangle), IMI (circle) and THI (rhombus) in live fungal cultures were indicated as open symbols, and control experiment using autoclave culture were indicate respective closed symbols. Values are means ± standard deviation of samples in triplicate.

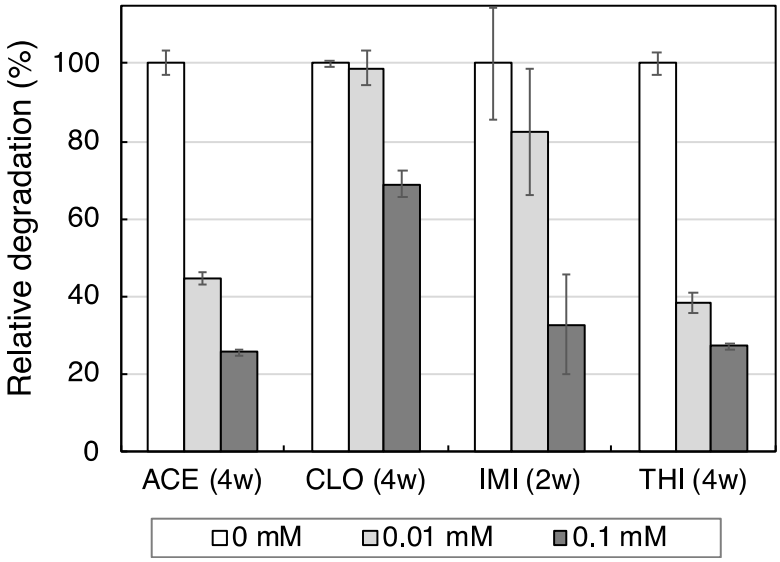


**Fig. 2. Inhibitory effect of a cytochrome P450 inhibitor, 1-ABT, on degradation of ACE, CLO, IMI and THI by *P. chrysosporium*.** 1-ABT and NEOs were added at the same time to pre-incubated culture of *P. chrysosporium*. After 4 weeks (for ACE, CLO and THI) or 2 weeks (for IMI) of incubation, residual amounts of NEOs were measured on HPLC. Values are means ± standard deviation of samples in triplicate.

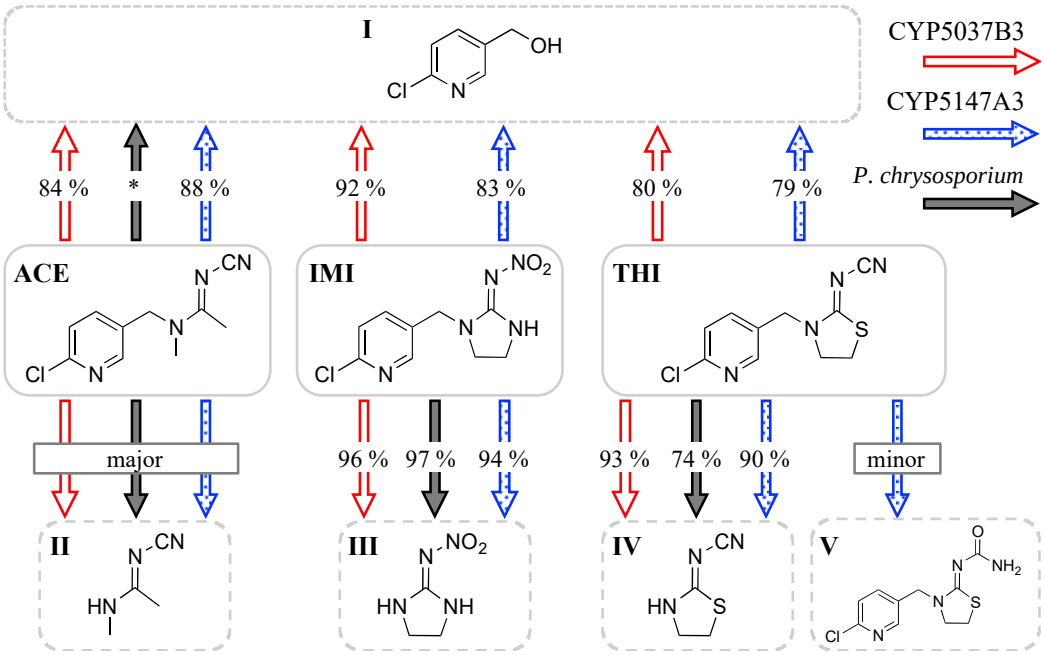


**Fig. 3. Schematic diagram of NEOs metabolic pathways in cultures of *P. chrysosporium*, or of yeast expressing CYP5037B3 or CYP5147A3.** Values express the transformation rate as calculated based on the amount of degraded NEOs and recovered metabolites. Asterisk indicates that the reaction was confirmed in previous work (Wang et al., 2019a).

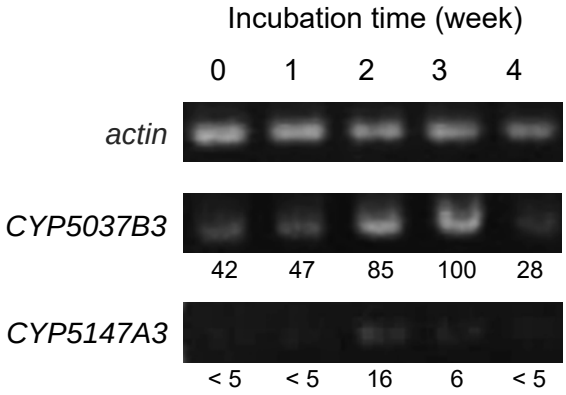


**Fig. 4. RT-PCR analysis of CYP5037B3, CYP5147A3, and actin expression in 0- to 4-week-old cultures of *P. chrysosporium*.** Values below images are relative expression levels of PcCYPs semi-quantified using actin as reference gene by ImageJ software (Abràmoff et al., 2004). Relative expression level is expressed by percentage of highest expression (CYP5037B3 expression at week 3).